ERDC/GSL TR-18-26

Geotechnical and Structures Laboratory

US Army Corps
of Engineers®
Engineer Research and
Development Center

ERDC
ENGINEER RESEARCH & DEVELOPMENT CENTER

Rapid-Setting Flowable Fill Performance in Cold Weather for Airfield Damage Repair

Lulu Edwards, William D. Carruth, Jeb S. Tingle,
and Isaac L. Howard

August 2018

The U.S. Army Engineer Research and Development Center (ERDC) solves the nation's toughest engineering and environmental challenges. ERDC develops innovative solutions in civil and military engineering, geospatial sciences, water resources, and environmental sciences for the Army, the Department of Defense, civilian agencies, and our nation's public good. Find out more at www.erdc.usace.army.mil.

To search for other technical reports published by ERDC, visit the ERDC online library at http://acwc.sdp.sirsi.net/client/default.

Rapid Airfield Damage Recovery (RADR) Program

ERDC/GSL TR-18-26
August 2018

Rapid-Setting Flowable Fill Performance in Cold Weather for Airfield Damage Repair

Lulu Edwards, William D. Carruth, and Jeb S. Tingle

Geotechnical and Structures Laboratory
U.S. Army Engineer Research and Development Center
3909 Halls Ferry Road
Vicksburg, MS 39180-6199

Isaac L. Howard

Materials and Construction Industries Chair
Mississippi State University, Civil and Environmental Engineering Department
501 Hardy Road, 235F Walker Hall, P.O. Box 9546
Mississippi State, MS 39762-9546

Final report

Prepared for U.S. Air Force Civil Engineer Center
139 Barnes Drive, Suite 1
Tyndall AFB, FL 32403

Under Project Number 397483

Abstract

This report documents the repair process of five craters in cold weather utilizing rapid-setting flowable fill (RSFF) and rapid-setting concrete (RSC). The work discussed herein supports the Rapid Airfield Damage Recovery (RADR) Program, in which the main objective is to develop capabilities to rapidly repair damaged airfield pavements for the full spectrum of operational scenarios. The purpose of this report is to document constructability, to collect early-age properties pertinent to the ability of these crater repair techniques to carry aircraft traffic, and to measure performance by exposing crater repairs to simulated aircraft traffic. Crater repair testing occurred at the Frost Effects Research Facility at the ERDC Cold Regions Research and Engineering Laboratory in Hanover, NH. Results showed RSFF could be a suitable cold-weather backfill. Aluminum sulfate was tested as an additive for use in cold weather, but repairs utilizing it did not perform well. The most efficient manner of using RSFF in cold weather was to heat the mix water. With heated mix water, a rapidly placed pavement repair was able to withstand 100 passes of an aircraft load cart after approximately 2 hr of cure time where RSFF was the backfill and RSC was the cap.

Contents

Abstract ii

Figures and Tables v

Preface vii

Unit Conversion Factors viii

1 Introduction and Background 1

1.1 Purpose and background 1

1.1.1 Purpose 1

1.1.2 Background 1

1.2 Objectives and scope 3

1.2.1 Objectives 3

1.2.2 Scope 3

1.3 Definitions and terminology 4

1.3.1 Definitions 4

1.3.2 Terminology 5

2 Experimental Program 8

2.1 Materials tested 8

2.2 Equipment 8

2.2.1 Compact track loader and attachments 9

2.2.2 Walk-behind saw 9

2.2.3 Wheeled skid steer 10

2.2.4 Pavement breaker 11

2.2.5 Excavator 11

2.2.6 Extendable boom forklift G6-42A 11

2.2.7 Simplified volumetric mixer 12

2.2.8 F-15E load cart 13

2.2.9 Heavy weight deflectometer 13

2.3 Facility 14

2.4 Experimental layout 16

2.5 Preparation and test sections 18

2.5.1 Saw cutting 18

2.5.2 Breaking and debris removal 20

2.5.3 Backfill placement 22

2.5.4 Cap placement 24

2.6 Data collection and trafficking 27

3 Test Results 32

3.1 Subgrade properties 32

3.2 Crater properties collected visually or via rod and level surveys 33

3.3 Heavy Weight Deflectometer (HWD) Test Results 38

3.4 Strength and setting assessments 39

4 Summary and Conclusions..46

References..47

Report Documentation Page

Figures and Tables

Figures

Figure 1. Caterpillar 279C CTL with Caterpillar SW45 wheel saw attachment. 9
Figure 2. Husquvarna 6600D saw. 10
Figure 3. Bobcat S250 wheeled skid steer. 10
Figure 4. John Deere 160C LC pavement breaker. 11
Figure 5. John Deere 135D excavator. 12
Figure 6. Gradall G6-42A extendable boom forklift. 12
Figure 7. Simplified volumetric mixer. 13
Figure 8. F-15E load cart. 14
Figure 9. Dynatest HWD. 14
Figure 10. CRREL FERF testing area. 15
Figure 11. FERF pavement prior to crater repairs - plan view. 15
Figure 12. FERF pavement prior to crater repairs - profile view. 16
Figure 13. Schematic profile view of Crater 1. 17
Figure 14. Saw cutting of Crater 1. 19
Figure 15. Example finished saw cut (Crater 1). 19
Figure 16. Existing pavement breaking process (Crater 1). 21
Figure 17. Debris removal and fully excavated Crater 1. 22
Figure 18. VMFF backfill placement photos (Crater 1). 23
Figure 19. RSC cap placement (Crater 1). 25
Figure 20. DPFF placement (Crater 5). 27
Figure 21. Density and moisture content measurement of subgrade. 28
Figure 22. Dynamic cone penetrometer testing of subgrade. 29
Figure 23. Temperature measurement within flowable fill. 30
Figure 24. Unconfined compression specimen fabrication. 30
Figure 25. F-15E traffic distribution. 31
Figure 26. Visual assessments from crater repair testing – Crater 1. 35
Figure 27. Visual assessments from crater repair testing – Craters 2 and 3. 36
Figure 28. Visual assessments from crater repair testing – Crater 4. 37
Figure 29. Visual assessment of Crater 5 just after placement. 38
Figure 30. Flowable fill temperature results. 40
Figure 31. DCP results (0- to 6-in. depth). 44
Figure 32. DCP results (6- to 12-in. depth). 45
Figure 33. DCP results (12- to 18-in. depth). 45

Tables

Table 1. FERF temperature log (May 29 to June 6, 2013). 16

Table 2. Summary of craters and their nominal dimensions. 17
Table 3. Saw cut lengths and properties. 20
Table 4. Subgrade density and moisture contents prior to crater placement. 32
Table 5. As-built crater dimensions. 33
Table 6. Visual assessments from crater testing. 34
Table 7. HWD test results. 39
Table 8. Material, water and air temperatures. 40
Table 9. VMFF backfill CBR values estimated from DCP testing. 42
Table 10. DPFF CBR values estimated from DCP testing. 43

Preface

This study was conducted for the U.S. Air Force (USAF) Civil Engineer Center (AFCEC) under the U.S. Air Force Rapid Airfield Damage Recovery (RADR) program. The technical monitor was Dr. Craig Rutland, AFCEC.

Besides the authors of this report, several individuals were involved in the efforts represented herein. Among them were Mr. Chase Bradley and Mr. Jay Rowland of the Geotechnical and Structures Laboratory (GSL) and Mr. Charlie Smith, Mr. Jared Oren, Mr. Glenn Durell, Mr. Charlie Schewela, Mr. T. J. Melendy, and Mr. John Severance of the Cold Regions Research and Engineering Laboratory (CRREL).

The work was performed through the Airfields and Pavements Branch (GMA) of the Engineering Systems and Materials Division (GM), U.S. Army Engineer Research and Development Center, Geotechnical and Structures Laboratory (ERDC-GSL) and the Engineering Resources Branch (RVE) of the Research and Engineering Division (RV), ERDC Cold Regions Research and Engineering Laboratory (ERDC-CRREL). At the time of publication, Dr. Timothy W. Rushing was Chief, CEERD-GMA; Mr. Jared I. Oren was Chief, CEERD-RVE; Dr. G. William McMahon was Chief, CEERD-GM; Mr. Jimmy D. Horne was Chief, CEERD-RV; and Mr. R. Nicholas Boone, CEERD-GVT, was the Technical Director for Force Projection and Maneuver Support. The Deputy Director of ERDC-GSL was Dr. William P. Grogan, and the Director was Mr. Bartley P. Durst. The Director was Dr. Joseph L. Corriveau.

COL Ivan P. Beckman was the Commander of ERDC, and Dr. David W. Pittman was the Director.

Unit Conversion Factors

Multiply	By	To Obtain
cubic feet	0.02831685	cubic meters
cubic yards	0.7645549	cubic meters
degrees Fahrenheit	(F-32)/1.8	degrees Celsius
feet	0.3048	meters
gallons (U.S. liquid)	3.785412 E-03	cubic meters
inches	0.0254	meters
inch-pounds (force)	0.1129848	newton meters
microinches	0.0254	micrometers
microns	1.0 E-06	meters
mils	0.0254	millimeters
ounces (U.S. fluid)	2.957353 E-05	cubic meters
pounds (force)	4.448222	newtons
pounds (force) per inch	175.1268	newtons per meter
pounds (force) per square inch	6.894757	kilopascals
tons (force)	8,896.443	Newtons
tons (2,000 pounds, mass)	907.1847	Kilograms

1 Introduction and Background

1.1 Purpose and background

1.1.1 Purpose

This report supports the Rapid Airfield Damage Recovery (RADR) Program, in which the objective is to develop capabilities to rapidly repair damaged airfield pavements for the full spectrum of operational scenarios including base recovery after an attack, expedient repairs at deployed locations, and sustainment of operating surfaces at forward operating bases. The U.S. Air Force (USAF) needs cutting-edge expedient repair technologies that can support cargo and fighter aircraft.

Over the past decade, the U.S. Army Engineer Research and Development Center (ERDC) has been working to improve RADR technologies beyond the capabilities of legacy solutions. One of the key activities towards that goal was the Critical Runway AssessmenT and Repair (CRATR) Joint Capabilities Technology Demonstration (JCTD) program, which includes three major technology demonstrations that are documented in Tingle et al. 2009, Priddy et al. 2013a, and Priddy et al. 2013b. The progression of using rapid-setting technologies is described in these documents. Early on were rapid-setting concrete (RSC) caps followed by rapid-setting flowable fill (RSFF) under RSC caps. Previous activities generally focused on more favorable conditions for rapid-setting materials, whereas this report documents an evaluation of RSFF in a cold-weather environment.

Cold weather is a potential impediment to the use of RSFF for RADR scenarios. The testing described in this report was designed to reflect the RADR concept of operations (CONOPS) and tactics, techniques, and procedures (TTPs).

1.1.2 Background

The objective of the RADR program is to modernize and streamline the ability of the USAF to rapidly repair damaged airfields for all different mission scenarios. The first mission scenario is the ability to recover a main operating base after an attack, including the requirement to be able to repair a small number of large craters created by conventional weapons as well as the requirement to repair a large number of small craters created by multiple warhead munitions. In a second scenario, USAF engineering forces are tasked with performing expedient repairs to open a base for initial operations after an attack, natural disaster, or seizure by friendly forces. This scenario requires the ability to deploy minimal assets and perform rapid repairs of a temporary nature to provide initial operational capability for a particular airfield. Once U.S. forces have established operations at a forward installation, the repair mission shifts to a sustainment mission where the objective is to perform maintenance and upgrades of the existing pavements to keep the airfield operational. Furthermore, in some deployed locations, it may become necessary to expand the operating surfaces to accommodate additional aircraft or to bypass severely damaged pavement sections.

Effective military airfield operations rely on several items. Optimal Maximum-On-Ground (MOG) capability is an important operational aspect and is the number of aircraft that can remain on the ground at any one time at a given airfield. MOG relates largely to force deployment and can be achieved in multiple ways, e.g., airfield matting as described in Anderton and Gartrell (2005) or through more efficient ADR activities.

In all of the aforementioned scenarios, time is a critical factor, either to restore flying operations or minimize airfield closures. The time required to return the airfield to operational status directly impacts the capability to launch and recover aircraft and meet air tasking order (ATO) requirements. Of comparable importance is the quality and durability of the repair or the number of aircraft passes sustained by a surface before repairs must be maintained or redone.

Previous research and development activities identified new materials, equipment, and processes for effectively repairing craters on the designated minimum aircraft operating surface (MAOS) runway/taxiway. The technical solutions were fully validated under realistic conditions during CRATR-JCTD activities. The Operational Utility Assessment (OUA) of the CRATR JCTD focused on the repair of several small craters. These same technologies are required in situations where the crater repairs are performed in inclement weather conditions, which is the focus of this report and where this report adds to the body of knowledge.

ERDC performed a cold-weather test of dry-placed flowable fill (DPFF) and RSC cap technology at Malmstrom AFB, MT, in March-April 2012

(Edwards et al. 2013). The wet-placement method of backfilling repairs with RSFF was not the focus of that test. The wet-placement method requires substantially more water for mixing than does DPFF. Overall, chemical admixtures, mixing equipment, and wet-placement repair processes such as volumetrically-mixed flowable fill (VMFF) need to be further evaluated for RSFF in cold weather conditions. To this end, the following objectives were established.

1.2 Objectives and scope

1.2.1 Objectives

The primary objective of the work described in this report was to evaluate the ability to perform wet placement, i.e., VMFF, of RSFF in freezing conditions and to measure subsequent performance with respect to early-age aircraft trafficking. Secondary objectives are listed below. In essence, this report evaluated repair materials, equipment utilized for making repairs, and cold weather TTPs.

1. Test aluminum sulfate ($AlSO_4$) at different dosage rates, heated water, and combinations of the two for their ability to facilitate use of RSFF under freezing conditions.
2. Identify modifications, e.g., admixture incorporation or heating mix water, to the simplified volumetric mixer that were evaluated in other facets of the ADR Modernization Program to improve its performance under sustained cold-weather conditions.
3. Identify any procedural modifications needed for performing crater repair tasks in sustained cold weather. This subtask evaluated equipment in terms of its ability to mix and place rapid-setting materials in cold-weather conditions for assessment TTPs.

1.2.2 Scope

The testing focused on evaluating materials, equipment, and procedures suitable for conducting cold weather repairs. Repairs were not conducted with USAF personnel, so timing and manpower analyses associated with multiple crater repairs were not conducted as a part of this report. A cold-weather demonstration using USAF personnel is documented in Edwards et al. (2013). The craters evaluated herein were constructed in the May-June 2013 timeframe at the Frost Effects Research Facility (FERF) at the ERDC Cold Regions Research and Engineering Laboratory (CRREL) in

Hanover, NH. This testing evaluated the effectiveness of current RADR technologies when repairs are required in sustained cold weather.

1.3 Definitions and terminology

This section contains terminology used throughout the report and also includes definitions that are central to the contents of this report. In most instances, these terms are defined upon first use and often re-defined at key locations within the report for ease of reading.

1.3.1 Definitions

1. *Rapid airfield damage recovery (RADR)*: Activities of engineer personnel in response to an attack on an airbase to provide adequate launch and recovery surfaces for the mission aircraft. Although RADR criteria were based on repairing airfields in friendly territory, recent military operations require repairing airbases occupied previously by hostile forces damaged during forcible entry or purposely sabotaged by departing forces. ADR encompasses other areas besides the repair of bomb damage including damage assessment, identification of candidate minimum operating strips, and the safe disposal of unexploded ordnance.
2. *Expedient repair*: Repairs conducted to create an initial operationally capable launch-and-recovery surface known as the minimum operating strip (MOS) based on projected mission aircraft requirements. These repairs are conducted in the most expeditious manner possible. When sufficient equipment and materials are available, individual crater repairs should be completed within 4 hr. Expedient repairs must provide an accessible and functional MOS that will sustain 100 passes of an F-15E aircraft with a gross single-wheel weight of 35,235 lb.
3. *Sustainment repairs*: Repair efforts to upgrade expedient repairs for increased aircraft traffic. These repairs are conducted as soon as the operational tempo permits and are expected to support the operation of at least 5,000 passes of an F-15E aircraft with a gross single-wheel weight of 35,235 lb without requiring additional maintenance. For these repairs, quality control is more important than construction time to minimize maintenance and maintain operational tempo.
4. *Rapid-Setting Flowable Fill (RSFF)*: A generic description of flowable fill that sets rapidly. Use of this term does not specifically define how the material was mixed and placed as any mixing and placement method would meet this definition.

5. *Dry-Placed Flowable Fill (DPFF)*: A specific placement method for RSFF that is placed into the crater without mixing outside the crater. The material is placed into the crater in relatively thin layers, e.g., 4 to 6 in., and water is added to the top of the thin layer but is not mixed.
6. *Volumetrically-Mixed Flowable (VMFF)*: A specific placement method for RSFF in which the material is volumetrically mixed outside the crater before placement. This material is continuously fed into the crater from the chute of a volumetric mixer and is also referred to as wet-placed flowable fill.
7. *Rapid-Setting Concrete (RSC)*: A concrete mixture making use of calcium sulfoaluminate (CSA) cement that has a setting time in normal conditions of approximately 30 min.

1.3.2 Terminology

Adj	Adjusted Deflection Measurements
AlSO4	Aluminum Sulfate
ATO	Air Tasking Order
CBR	California Bearing Ratio
CONOPS	Concept of Operations
CLSM	Controlled Low-Strength Material
CRATR	Critical Runway AssessmenT and Repair
CRREL	Cold Regions Research and Engineering Laboratory
CSA	Calcium Sulfoaluminate Cement
CTL	Compact Track Loader
D	Deflection
D1 to D7	Deflection Measured at 1-ft Intervals from Load
DoD	Department of Defense

DPFF	Dry-Placed Flowable Fill
ERDC	Engineer Research and Development Center
FERF	Frost Effects Research Facility
FF	Flowable Fill
FOD	Foreign Object Debris
HWD	Heavy Weight Deflectometer
JCTD	Joint Capabilities Technology Demonstration
MAOS	Minimum Aircraft Operating Surface (MAOS)
MEF	Material Evaluation Facility
MOG	Maximum-on-Ground
OCL	Overcut Length
OUA	Operational Utility Assessment
PCC	Portland Cement Concrete
RADR	Rapid Airfield Damage Recovery
RSC	Rapid-Setting Concrete
RSFF	Rapid-Setting Flowable Fill (VMFF, DPFF, or other)
SME	Subject Matter Expert
SVM	Simplified Volumetric Mixer
SW	Single Wheel
T_{FF}	Flowable Fill Temperature

TTPs	Tactics, Techniques, and Procedures
UCS	Unconfined Compressive Strength
U.S.	United States
USACE	United States Army Corps of Engineers
USAF	United States Air Force
VMFF	Volumetrically-Mixed Flowable Fill
p-c	Pass to Coverage Ratio
t_{set}	Setting Time
w/c	Water-to-Cement Ratio by Mass
^{o}F	Degrees Fahrenheit

2 Experimental Program

Craters were generated mechanically inside the FERF. Testing was performed under controlled conditions to evaluate technologies and processes. The crater repairs were performed under sustained freezing conditions, specifically ambient temperatures below 32°F and ground frost depths of approximately 3 ft. Relevant experimental activities were performed between 28 May and 6 June 2013.

2.1 Materials tested

Three materials were evaluated during this testing program. In addition to these materials, a few incidental materials, e.g., Durabase mats that were not directly part of the experiments, were used to facilitate experiments.

1. Utility Fill 1-Step 750: Forty-eight super sacks (3,000 lb each) of RSFF were needed for these experiments. This material was produced by Buzzi Unicem USA Inc. and was composed of silica sand, several calcium silicates, aluminous materials, and gypsum. General characteristics included an initial set strength of around 250 psi after 30 min in normal conditions. The RSFF contains calcium sulfoaluminate (CSA) cement.
2. CTS Rapid Set Concrete Mix®: Twenty-two super sacks (3,000 lb each) of RSC were needed for these experiments. This material is produced by CTS Cement and is referred to as Rapid-Set Concrete Mix®, AC Concrete Mix. The main cementitious component of this mix is rapid-set cement, which is a proprietary CSA cement. The set time of this material is approximately 30 min, and the mix contains 3/8-in. maximum-sized aggregates.
3. Aluminum Sulfate: Aluminum sulfate ($AlSO_4$) was selected for use in the mix water as an accelerator for RSFF and/or RSC in this effort, based on laboratory work by Oren et al. (2014). The granulated material was packaged in 50-lb plastic sacks.

2.2 Equipment

Key equipment utilized during this work is described in the following sub-sections. Some details such as equipment specifications have been omitted, though many are readily available in Carruth and Howard (2016). In addition to the equipment listed, ERDC representatives utilized their

ADR tool container, which features several fundamental items used during crater production, repair, and/or testing. Since the focus of this test was the effects of cold weather on repair materials, standard ADR equipment was not utilized in all cases.

2.2.1 Compact track loader and attachments

A Caterpillar 279C compact track loader (CTL) was used with different attachments during these efforts. This CTL, i.e., skid steer, has quick-disconnect fittings for changing attachments that expedite the ADR process. For ADR, a CTL serves multiple purposes including rapidly cutting around upheavals, removing debris, and cleaning (different attachments are used for each purpose). Attachments used for this project included a multi-purpose bucket and angle broom attachment for debris removal, a Caterpillar SW45 wheel saw for cutting, and a fork attachment for material handling. Figure 1 shows the 279C with the wheel saw attachment.

Figure 1. Caterpillar 279C CTL with Caterpillar SW45 wheel saw attachment.

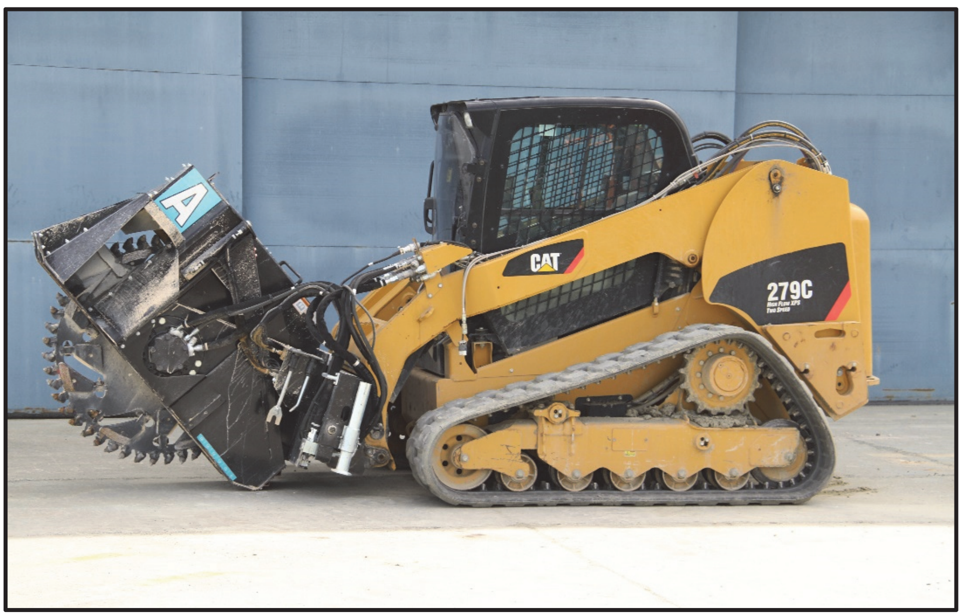

2.2.2 Walk-behind saw

A Husqvarna 6600D walk-behind saw, shown in Figure 2, was used for making some saw cuts during crater repair activities. A 36-in.-diameter blade was used that typically made a 6-in.-deep cut first, followed by a full-depth cut. The walk-behind saw was used for the transverse cuts because of the space limitations due to the concrete walls, preventing the wheel saw from being used.

Figure 2. Husquvarna 6600D saw.

2.2.3 Wheeled skid steer

A Bobcat S250 wheeled skid steer was used for various purposes and is shown in Figure 3. One purpose was breaking out existing material so the repairs could be excavated; another purpose was to move material using a bucket attachment.

Figure 3. Bobcat S250 wheeled skid steer.

2.2.4 Pavement breaker

The John Deere 160C LC excavator equipped with a pavement breaker, shown in Figure 4, was used to break material within the crater boundary into fragments so it could be removed prior to excavation.

Figure 4. John Deere 160C LC pavement breaker.

2.2.5 Excavator

The John Deere 135D excavator equipped with a bucket, shown in Figure 5, was used primarily for debris removal from craters after the material had been broken into fragments.

2.2.6 Extendable boom forklift G6-42A

The forklift shown in Figure 6 was used to handle super sacks of RSFF and RSC throughout the crater repairs. In some cases, the super sacks were placed into the volumetric mixer described in the next section and, in other cases, they were placed directly into the crater to be repaired.

Figure 5. John Deere 135D excavator.

Figure 6. Gradall G6-42A extendable boom forklift.

2.2.7 Simplified volumetric mixer

The simplified volumetric mixer (SVM), shown being loaded with super sacks in Figure 7, was used to place the majority of the RSFF and RSC into the five crater repairs. A 2,000-gal water truck (not shown) was also utilized to refill the water tanks on the SVM as needed. The SVM consisted of a single dry-material hopper with a 6-yd^3 capacity, a conveyor belt feed system, a positive displacement water pump, water tanks, and a mixing auger. The water-to-cement (w/c) ratio was controlled by way of a strike-off gate for the dry-material conveyor. The SVM was calibrated to deliver a desired amount of water for a given amount of dry flowable fill, e.g., 70 gal of water per 3,000 lb super sack of flowable fill. The SVM can produce VMFF or RSC, is towed behind a vehicle, and was equipped with water heaters for these crater repairs. Carruth and Howard (2016) contains additional information about the SVM.

The SVM was modified for this project by fitting the water system with immersion heaters and pipe heating cables that allowed heated water to be utilized for VMFF. Immersion heaters were selected, spacers were fabricated, and heating times were tested to verify that the desired water temperatures could be achieved.

Figure 7. Simplified volumetric mixer.

2.2.8 F-15E load cart

The F-15E load cart shown in Figure 8, representing a single-wheel load of 35,325 lb at a 325-psi tire pressure, was used to apply simulated aircraft traffic on the surface of each completed crater repair.

2.2.9 Heavy weight deflectometer

The Dynatest heavy weight deflectometer (HWD) shown in Figure 9 was used to assess repaired crater stability before, during, and after trafficking.

Figure 8. F-15E load cart.

Figure 9. Dynatest HWD.

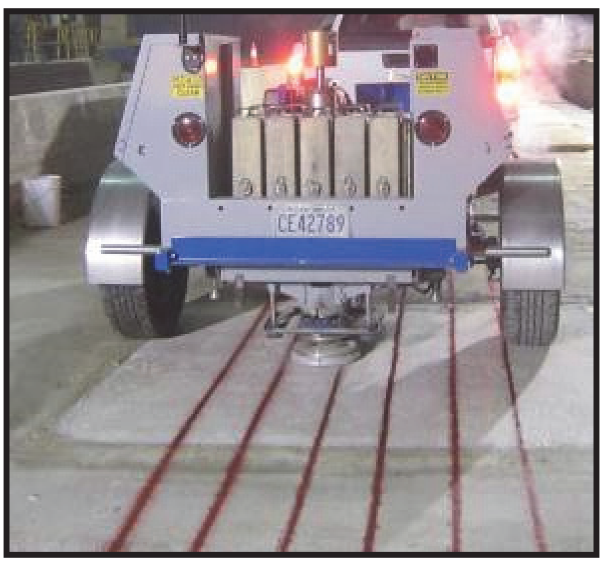

2.3 Facility

Testing was performed in the Frost Effects Research Facility (FERF) of ERDC's Cold Regions Research and Engineering Laboratory (CRREL) in Hanover, NH. Figure 10 shows a photograph of the testing area.

Figure 10. CRREL FERF testing area.

To begin these experiments, the FERF had testing quadrants that were 100 ft long by 21 ft wide. The quadrants featured 60 ft of portland cement concrete (PCC) roadway with a nominal 5 ksi compressive strength divided evenly into three 20-ft-long by 18-ft-wide slabs. This pavement section was bound by concrete retaining walls. Underneath the PCC was crushed limestone with a California Bearing Ratio (CBR) of approximately 80 that rested on a silt foundation (or subgrade) where the CBR was less than 10. Note that these CBR values are in an unfrozen condition and are for general information only. On each side of the 60-ft-long concrete roadway was 20 ft of crushed stone. Figures 11 and 12 document the pavement plan and profile views where craters were later produced and repaired. Table 1 summarizes temperature and frost depth conditions within the facility during the testing activities documented herein.

Figure 11. FERF pavement prior to crater repairs - plan view.

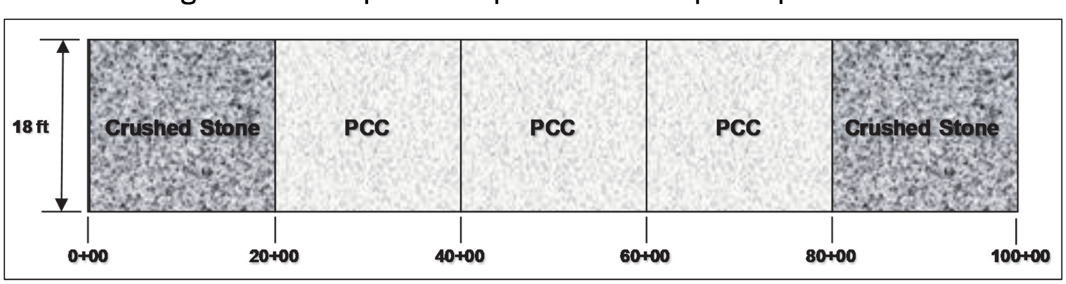

Figure 12. FERF pavement prior to crater repairs - profile view.

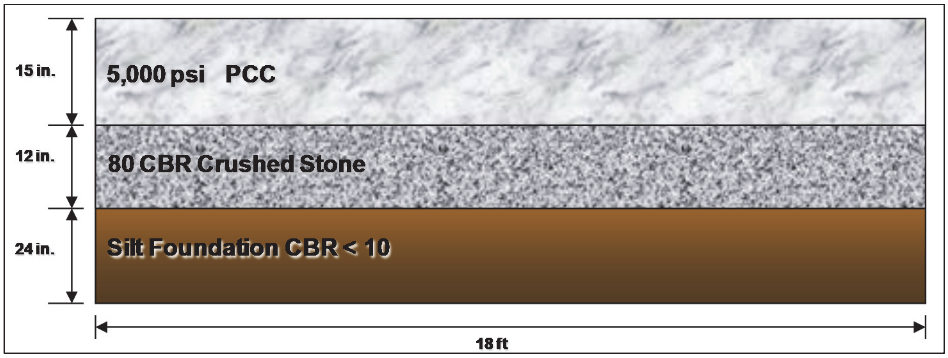

Table 1. FERF temperature log (May 29 to June 6, 2013).

Date	Time	Surface Temp (°F)	6-in. Depth Temp (°F)	18-in. Depth Temp (°F)	Frost Depth (in.)
May 29	9:00 AM	37	---	---	36
May 30	2:00 PM	38	-5	-9	36
May 31	8:00 AM	35	-4	-5	36
May 31	10:30 AM	38	-5	-5	36
May 31	1:45 PM	41	-4	-5	36
May 31	5:00 PM	43	-2	-4	36
June 01	7:15 AM	34	-1	-2	36
June 02	6:00 AM	30	-1	-1	36
June 02	8:20 AM	33	-1	-1	36
June 02	11:00 AM	36	0	-1	36
June 04	11:00 AM	30	1	1	36
June 04	2:00 PM	29	1	1	36
June 06	7:15 AM	22	1	1	36

2.4 Experimental layout

Table 2 summarizes relevant properties of the five crater repairs; nominal dimensions are provided in this section, and as-built dimensions are provided later in the report. The backfill and capping material columns summarize water temperature, RSFF technique (VMFF or DPFF), and $AlSO_4$ dosage. All water was heated with the immersion heaters added to the SVM that are described in Section 2.2.7. No additives were used to heat the mix water, though they have been investigated in other laboratory works by ERDC (e.g., Oren et al. 2014).

Table 2. Summary of craters and their nominal dimensions.

Crater	Nominal Size (ft)	Nominal Crater Depth (in.)	Proposed Backfill Material	Proposed Capping Material
1	6 x 6	32	22-in. VMFF w/ no additives and 57 °F H_2O	10-in. RSC w/ no additives and 57 °F H_2O
2	7 x 7	32	22-in. VMFF w/ 1.1% $AlSO_4$ and 52 °F H_2O	Did not cap – VMFF didn't set
3	7 x 7	32	22-in. VMFF w/ no additives and 80 °F H_2O	10-in. RSC w/ no additives and 57 °F H_2O
4	8 x 8	32	22-in. VMFF w/ 0.5% $AlSO_4$ and 87 °F H_2O	10-in. RSC w/ no additives and 57 °F H_2O
5	7 x 9	32	12-in. VMFF w/ no additives and 91 °F H_2O	20-in. DPFF w/ no additives and 50 °F H_2O

Craters 1 to 4 were produced in the middle PCC slab seen in Figure 11. Figure 13 shows a general example for Crater 1. All four of these craters were in the same location due to the FERF's restricted space and the desire for early-age trafficking. Note that, as shown in Table 2, craters increase in size due to the need to saw-cut a new crater each time.

Figure 13. Schematic profile view of Crater 1.

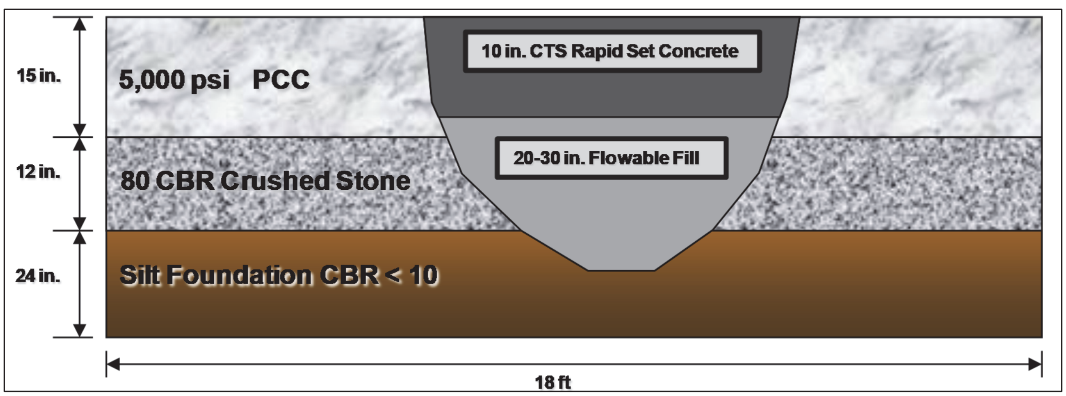

After producing the fourth crater, it was decided that a new location was needed for the fifth crater since the middle slab had been worn from the four craters already evaluated. Therefore, the north end PCC slab was used for Crater 5. Since this slab was on one end of the section, trafficking did not occur due to space restrictions; it was for constructability and property measurements only. Craters were prepared and repaired in serial order.

Although DPFF is typically used when the repair is surfaced with rapid-setting concrete (RSC), the combination of VMFF backfill and an RSC cap was used in four of the five craters to measure performance of this combination under cold weather conditions. The fifth crater was only to assess the ability to place DPFF in sustained cold weather conditions; the crater repair was not capped with RSC. Repair materials were conditioned, and the repairs were conducted at temperatures sustained below 32°F. Air temperatures measured during and adjacent to crater repairs were 27 to 31°F, with values measured as high as 33°F at other locations in the FERF.

2.5 Preparation and test sections

In preparation for test-section activities, aggregates were placed at the ends of Durabase mats, and existing slabs were rod- and level-surveyed. Each crater was repaired according to the following steps: 1. saw-cutting the pavement surface; 2. breaking up and removing the material inside the saw cut; 3. backfilling the prepared excavation with VMFF; and 4. capping the surface with either RSC or DPFF. Pertinent details from each of these steps are described in the remainder of this section.

2.5.1 Saw cutting

Boundary lines were first painted for saw cutting. Figure 14 provides photos of the saw-cutting process, while Figure 15 shows a completed saw cut. Saw-cutting provided the crater's boundary lines. Table 3 provides approximate information about the saw-cut crater boundary lines. Note that saw-cut lengths would generally be larger than actual crater dimensions.

Figure 14. Saw-cutting of Crater 1.

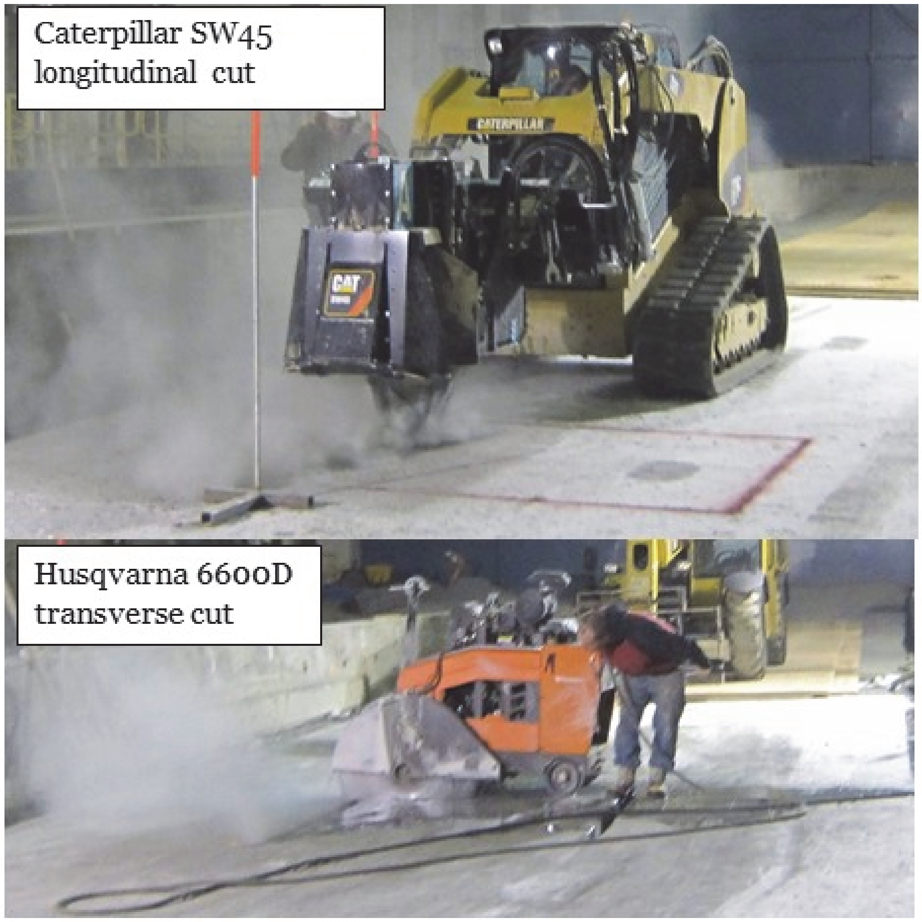

Figure 15. Example of finished saw cut (Crater 1).

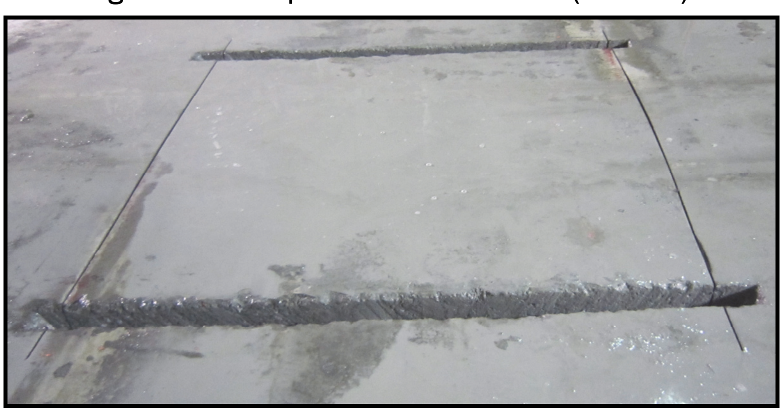

Table 3. Saw-cut lengths and properties.

Crater	Cut Lengths (in.)				OCL Range
	L1	L2	T1	T2	(in.)
1	79	80	84	84	3 to 7
2	92	90	83	82	3 to 6
3	92	90	83	82	3 to 6
4	94	94	96	92	3 to 10
5	89	87	106	102	5 to 15

--Beginning in southwest corner of a crater and first heading north, then east, south, and west, are L1, T1, L2, and T2.

--OCL is overcut length. OCL range is the maximum and minimum OCL values for a given crater.

--Typical cut widths for L1 and L2 were around 3 in., and typical cut widths for T1 and T2 were around 0.25 in.

Longitudinal (east-west) cuts (L1 and L2) were made with the CTL Caterpillar 279C-SW45 utilizing Caterpillar 149-5763 model teeth. Some cuts with the wheel saw were modestly delayed from the CTL slipping on ice. Transverse (north-south) cuts (T1 and T2) were made with the Husqvarna 6600D, which introduced considerable water into the cuts. Each transverse and longitudinal cut took on the order of 5 to 10 min.

2.5.2 Breaking and debris removal

Initial attempts were made in Crater 1 to break out the sawn crater with a Bobcat S250 wheeled skid steer (Figure 3) with a pavement breaker attachment. After approximately 20 min, this approach was deemed minimally effective; the slab had been broken 11 times on the north edge at this point. Thereafter, a John Deere 135D excavator (Figure 5) with a hammer attachment was used; the slab was broken 14 times with this approach. Visually, the slab seemed harder than normal to break and also seemed very flaky near the top (broke into several small pieces). The crater was then excavated to a depth of approximately 32 in. with a John Deere 135D with a 36-in.-wide bucket and 7-in.-long teeth. Figure 16 summarizes the breaking process ultimately used for Crater 1, and Figure 17 shows debris removal and the completed Crater 1.

Figure 16. Existing pavement breaking process (Crater 1).

For Crater 2, the breaking hammer was operated at full speed on the RSC cap (3 breaks). To break the VMFF backfill, 16 breaks occurred. Debris was removed with a bucket, and there was some difficulty removing material because the edges and corners were not completely severed off. The corners still had modest amounts of material attached, which was removed with a chipping hammer. For Crater 3, no breaking was necessary since the RSFF did not set (more information in the next section). For Crater 4, a John Deere 160C LC (Figure 4) with a hammer attachment was used to break the existing pavement. After breaking, the material inside the cuts was removed with a John Deere 135D tracked excavator to a depth of approximately 33 in.

Figure 17. Debris removal and fully excavated Crater 1.

2.5.3 Backfill placement

Prior to backfill placement, a reference line was painted at a depth of 10 in. for craters where RSC was to be placed. To place VMFF, the SVM was loaded with four super sacks of material that were handled with a G6-42A forklift (Figure 6). A release agent was used on the mixer prior to beginning RSFF placement. Figure 18 provides photos of VMFF placement as backfill.

Figure 18. VMFF backfill placement photos (Crater 1).

Crater 2 was placed in approximately 13 min with an initial gate setting of 4.5, but the material appeared wet. The gate was moved to 5.0 and then 5.5. $AlSO_4$ appeared to reduce Crater 2's free water, and the gate was lowered back to 5.0, at which the material had a milkshake consistency. Although it did not flow completely freely, it was easily moved with concrete rakes. Crater 2 utilized 33 lb of AlSO4 and 75 gal of water per super sack of flowable fill. The material did not set, likely due to the AlSO4 additive, and was excavated without receiving a surface cap.

Once the VMFF from Crater 2 was excavated, Crater 3 was placed in the same excavated area without the need for saw-cutting or breaking of the crater repair material. Crater 3 utilized SVM gate settings of 4.5 to 5.5. For a few brief durations, material exiting the mixer appeared dry, since the gear driving the water pump temporarily became disengaged.

Crater 4 utilized approximately 124 ft^3 of VMFF (6 supersacks) with 0.5% $AlSO_4$ (75 lb of $AlSO_4$ per 400 gal of water). The VMFF was placed with a strike-off gate setting of 4.5 to 5.0. At one instance, it was noted that the RSFF looked dry. Placement of DPFF for Crater 5 appeared normal.

2.5.4 Cap placement

To place RSC caps, the SVM was loaded with 3 super sacks of material. $AlSO_4$ was considered for use within RSC, but since RSC worked well without any additives in the previous cold-weather test, it was not incorporated into any of the crater repair caps. Prior to mixing, a release agent was applied to the SVM auger, hand tools, and screed.

Crater 1 RSC was placed in approximately 10 min. This material was vibratory screeded twice, and the edges were cleaned. At the time of screeding, material temperatures were around 35°F, and ambient inside temperatures were around 33°F. Some excess water/paste was skimmed from the surface to minimize shrinkage cracking potential and optimize cleanliness. The surface of RSC material can be torn by over-finishing, and tears show up as cracks in the completed repair. Minimal finishing activities should occur, and they should occur very quickly after placement. Figure 19 provides example photos of RSC cap placement.

Figure 19. RSC cap placement (Crater 1).

Crater 3 was placed with a gate setting of 4.5 to 5.5 (mostly 5.0). The cap's edges were finished by placing a trowel on end to mark the edge and remove excess material after vibratory screeding twice. During placement, there was some excess water removed from the crater. After placement, some shrinkage cracking was observed toward the center of the repair. The shrinkage cracking was not believed to be especially problematic, but it was more than was observed in Crater 1. Overall, the surface was smooth. Crater 4 was placed with a gate setting of 5.

Crater 5 was not capped with RSC; instead, approximately 20 in. of DPFF was placed to evaluate the properties of DPFF in a controlled environment. Figure 20 shows summary photos of DPFF cap placement. There were approximately 4.75 super sacks of dry material utilized. Approximately 5 gal of water were introduced into the crater ahead of the first super sack that had 75 gal of water placed over it. The second super sack also had 75 gal of water applied to it, while the third and fourth super sacks had only 60 gal of water each. Only 75% of the fifth super sack was used, and an additional 20 gal of water was placed on the surface for a total of 295 gal of water. Less water is typically used for the final super sack to reduce surface moisture, which can remain even after the material has set. Finishing occurred with an aluminum bar, and the surface was bull-floated and worked with hand tools for approximately 7 min.

Figure 20. DPFF placement (Crater 5).

2.6 Data collection and trafficking

Generally speaking, data collection for each repair consisted of material properties, layer thicknesses, visual observations, overall crater stability, and ability to carry simulated aircraft traffic at early ages. Data collection occurred before, during, and after crater repairs. Event logs were kept by at least one subject matter expert throughout data collection, and these logs were used during generation of this report. These logs contained temperature, timing, personnel, and other potentially relevant information. While on site, subjective visual assessments were also part of data collection. These visual assessments documented repair damage (spalling, cracks, ruts, and similar) during and after trafficking. Visual damage was often highlighted with paint and photographed.

After craters were sawed and the debris excavated, water and dry material temperatures were recorded periodically as needed. When measuring water temperatures, the location of the thermometer within the SVM water supply tank had a considerable effect on the results. A reasonably representative value was recorded as the mix water temperature.

After debris excavation, a Troxler 3440 nuclear gage (Figure 21) was used to collect subgrade density and moisture content data per ASTM C2922 (ASTM 2004a) and D3017 (ASTM 2004b), respectively. Rod and level measurements were also taken on the subgrade alongside dynamic cone penetrometer (DCP) measurements (Figure 22), which were used to estimate California Bearing Ratio (CBR) values per ASTM D6951 (ASTM 2009).

Figure 21. Density and moisture content measurement of subgrade.

Figure 22. Dynamic cone penetrometer testing of subgrade.

After placement of the VMFF backfill, additional DCP measurements were obtained over time for CBR estimation, and another rod and level survey was conducted to measure as-built layer thickness. Temperature was also measured within the as-placed VMFF in some instances (e.g., Figure 23) and denoted T_{FF}. Measurements were obtained a considerable distance from crater edges. Figure 24 shows cylindrical specimens being molded adjacent to the pavement repair. These specimens were collected in an attempt to obtain strength and set-time data on the VMFF as it was placed. Material samples from which molded specimens were made were usually taken directly from the mixer chute. Some of the molded specimens were left in the FERF facility, while others were transferred to an even colder location referred to as the Material Evaluation Facility (MEF) to assess how well small specimens handle very cold surrounding temperatures during early-age property development. These specimens were tested for set time via ASTM C403 (2008) (test times were altered from recommended values) where a value of 500 psi was denoted (t_{set}) and unconfined compressive strength (UCS) according to ASTM C39 (2012).

Figure 23. Temperature measurement within flowable fill.

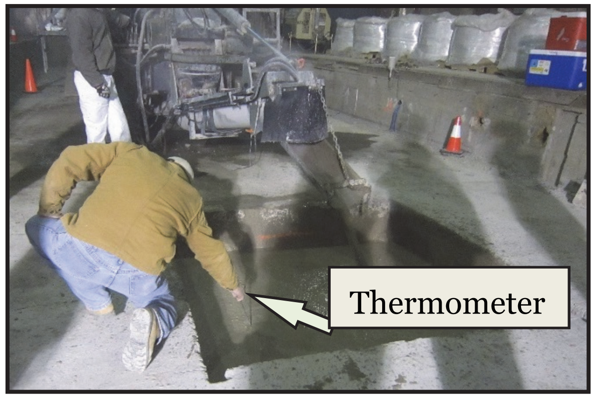

Figure 24. Unconfined compression specimen fabrication.

A rod and level survey was performed on the completed RSC caps after approximately 1.5 hr. Thereafter, for Craters 1 to 4, HWD measurements were obtained just before F-15E trafficking, i.e., at approximately 2 hr, and again immediately after 112 passes of the F-15E load cart were applied as described in the following paragraph. HWD testing was performed at two curing time intervals for Crater 5, since it was not trafficked.

HWD data were collected primarily to characterize the stiffness of a given repair, investigate trends, and provide an independent behavioral assessment. HWD testing measured deflection (D) at seven locations (D_1 to D_7) relative to the center of the load plate on 12-in. intervals where D_1 was under the center of the load. The HWD load plate was 11.8-in. in diameter, with most testing being on the order of 500 psi (55 kips). Deflection measurements were linearly adjusted to a contact stress and referred to as *Adj* alongside the value to which measurements were adjusted (200 psi or 500 psi).

The default traffic application consisted of 112 passes of an F-15E load cart (see Section 2.2.8) immediately after placement, since achieving 100 or more passes after 2 hr of cure time is a critical threshold for RADR base recovery scenarios. Figure 25 shows the traffic pattern used to approximate a normally distributed traffic sequence across the repairs. Each pattern applied 16 passes in a normal distribution, with a pass-to-coverage ratio of 4. Within one pattern, the first two passes of the single-wheel load cart traveled along the path labeled “1 2,” then the load cart shifted over into the path labeled “3 4 15 16” and made passes 3 and 4. The remaining passes were made in order with the load cart completing the pattern in the path labeled “3 4 15 16” by making passes 15 and 16. This pattern of 16 passes was repeated 7 times. Traffic was applied to Craters 1 to 4 individually, and traffic began approximately 2 hr after the surface cap was placed on each repair.

Figure 25. F-15E traffic distribution.

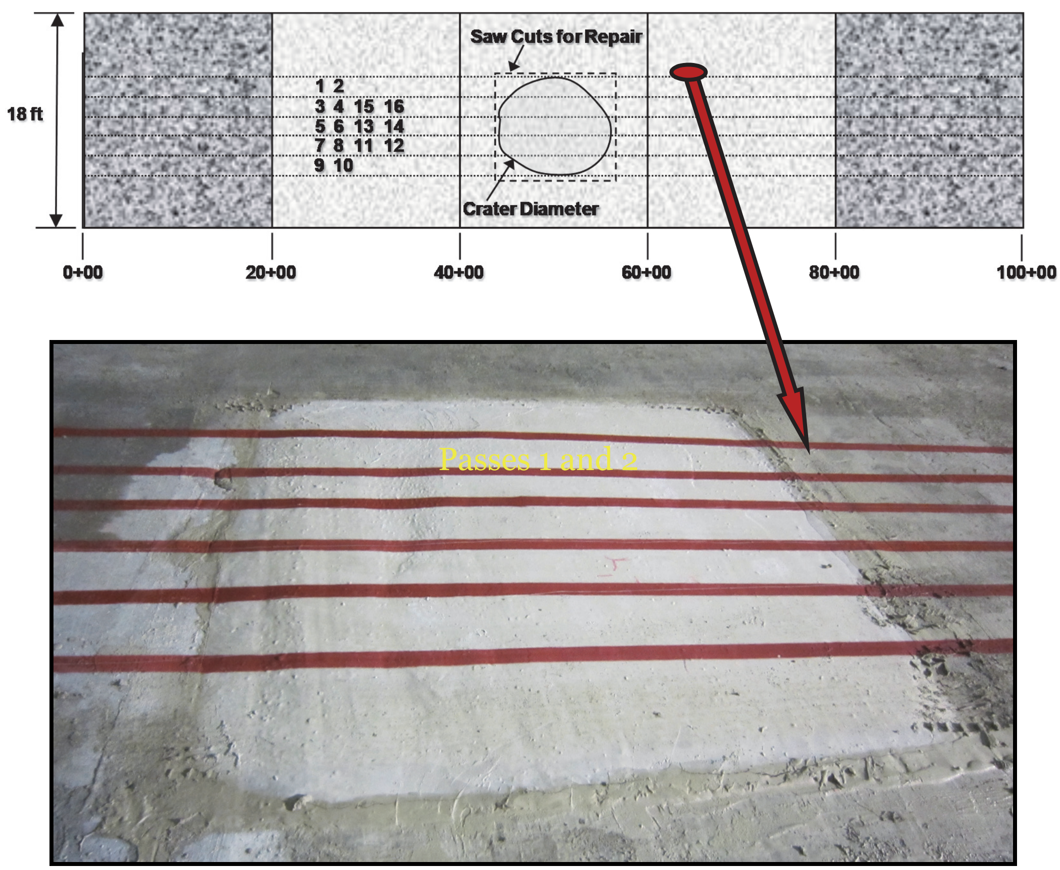

3 Test Results

Results are divided into four sections. First, subgrade properties were reported, as they are a reference for crater repair performance assessments. Thereafter, overall performance of the crater repairs was reported as assessed visually and with rod and level measurements. The remaining two sections discuss setting, strength, and/or stability properties to explain what led to the overall performance assessment observed.

3.1 Subgrade properties

Table 4 summarizes in-place subgrade density and moisture contents for the silt subgrade obtained from nuclear gauge measurements. Average values are italic and in parenthesis. Table 4 shows that re-use of the same location for Craters 1 to 4 led to progressive reductions in dry density and increases in moisture content. The reported values are not of concern relative to the project's objectives but are noteworthy.

Table 4. Subgrade density and moisture contents prior to crater placement.

Crater	Dry Density (pcf)	Wet Density (pcf)	Moisture Content (%)
1	109.5, 112.9, 112.4 *(111.6)*	116.8, 119.9, 120.3 *(119.o)*	6.6, 6.2,7.0 *(6.6)*
2	112.5, 106.4, 114.0 *(111.0)*	120.9, 119.2, 125.5 *(121.9)*	7.4, 12.0, 9.3 *(9.6)*
3[a]	112.5, 106.4, 114.0 *(111.0)*	120.9, 119.2, 125.5 *(121.9)*	7.4, 12.0, 9.3 *(9.6)*
4	110.0, 109.9, 98.6 *(106.2)*	130.5, 128.4, 121.3 *(126.7)*	18.6, 16.8, 22.7 *(19.4)*
5	112.0, 109.3, 109.0 *(110.1)*	127.1, 125.1, 125.9 *(126.0)*	13.5, 14.5, 15.5 *(14.5)*

[a]Nuclear gauge data were not obtained for Crater 3 but were taken to be the same as Crater 2 since the same excavation was used.

DCP measurements showed the subgrade of Crater 1 with CBR values of approximately 100. Crater 2's CBR values decreased relative to Crater 1 and were highly variable, from 2 to 100. Crater 3 was taken to be the same as Crater 2, since Crater 2 was not trafficked. Crater 4 CBR values were further reduced to an average of 30 (range of 8 to 60). Crater 5 CBR values were comparable to Crater 1 at approximately 100 for the upper 20 in. (values decreased somewhat at depths greater than 20 in.)

Two noteworthy observations were made with subgrade DCP data. First, CBR values were higher than the typical non-frozen value of less than 10 presented earlier for this silty material. This is likely due to the subgrade being frozen at the time of DCP testing. Second, although measured values were erratic, the lowest distribution of values was measured in Crater 4, which also had the lowest dry density and highest moisture content. As with density alone, DCP values indicate some differences in subgrade properties, but these differences are not believed to have affected the overall objectives of this project.

It should be noted that the subgrade CBR conditions at the time of trafficking may not be fully represented by these tests. Moisture from the VMFF, and especially heat generated from the VMFF, could reduce CBR values relative to those measured by the DCP when the backfill was not present.

3.2 Crater properties collected visually or via rod and level surveys

Table 5 provides as-built crater properties with average thicknesses from rod and level survey measurements. Table 6 and Figures 26 to 29 provide visual assessments of all five crater repairs tested with an F-15E aircraft load alongside two examples of newly completed craters. A key observation was that all crater repairs that were trafficked (Craters 1, 3, and 4) were able to withstand 112 passes of the F15-E load cart.

Table 5. As-built crater dimensions.

Crater	Actual Size (ft)	Backfill Thickness (in.)	Cap Thickness (in.)	Actual Crater Depth (in.)
1	5.9 x 6.0	21.1	8.3	29.4
2	7.0 x 6.9	[a]---	[a]---	[a]---
3	7.0 x 6.9	21.7	8.8	30.5
4	7.8 x 7.9	22.0	9.4	31.4
5	7.3 x 8.7	10.4	22.4	32.8

[a]Measurements were not obtained for Crater 2 since RSFF did not set.

The $AlSO_4$ additive did not perform well when used by itself to accelerate the chemical reaction of VMFF. Crater 2 did not set up at all, which was considered a failure that led to this material being removed before a cap was placed.

No structural failures occurred for the crater repairs that were trafficked, implying that VMFF capped with RSC was adequate for the as-placed thicknesses. As with other crater repairs, repair edges are the likely failure mode since there is no load transfer at the edge. This is especially true in cold regions as the lower temperature pavement surrounding the crater is going to reduce curing temperatures near the edges, weakening the system in this region at early ages.

Table 6. Visual assessments from crater testing.

Crater	Before Traffic	During or After Traffic
1	Steam was visible during RSC placement. Very minor shrinkage cracking in the crater repair's center, along with typical hairline cracks around the perimeter. The RSC around the edges was soft enough 2 hr after placement that it was imprinted by the HWD truck tires and load cart tires.	There was no additional cracking after trafficking or due to temperature exposure overnight. Trafficking led to minor edge spalling due to excess material overlap.
2	Backfill did not set after 2.5 hr, so crater repair was discontinued.	No traffic applied
3	Minor shrinkage cracking was observed on the surface prior to trafficking due to wet paste resulting from a temporary partial clog of the conveyor belt due to a conglomerate of RSC lodged at the strike-off gate.	There was little to no change in condition due to trafficking. No additional cracking or Foreign Object Debris (FOD) was observed.
4	Typical edge cracking and minor shrinkage cracking occurred where the crater was over finished. No problems were observed with setting, but curing did appear to be slower around the edges where the mix was in contact with the cold existing pavement. An estimated 1 to 2 in. around the perimeter was less cured due to colder interface temperatures.	There was no additional cracking as a result of trafficking, but there was minor expansion observed in the small shrinkage cracks.
5	There were no major problems placing DPFF as a cap over VMFF backfill.	No traffic applied

Figure 26. Visual assessments from crater repair testing – Crater 1.

Figure 27. Visual assessments from crater repair testing – Craters 2 and 3.

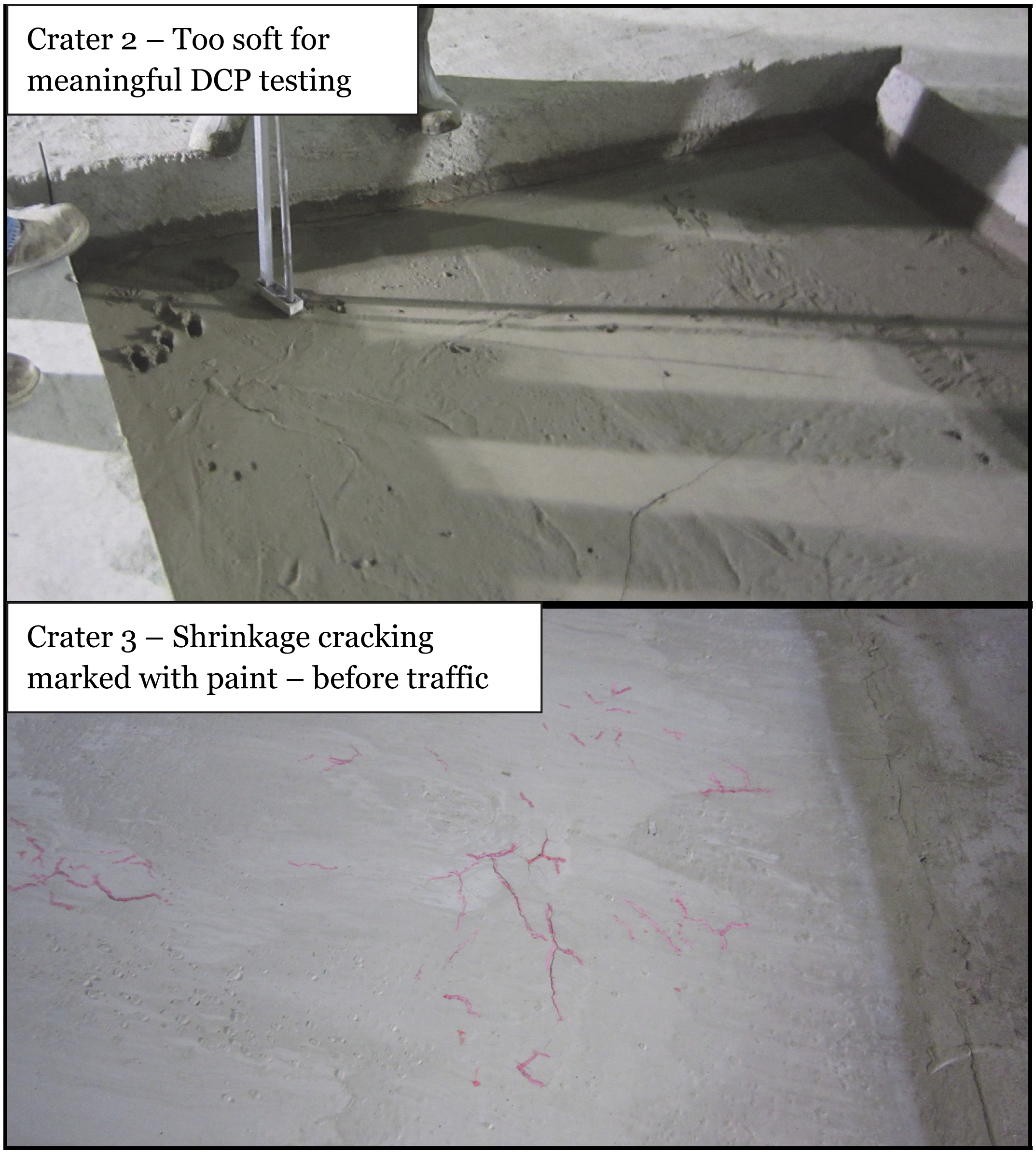

Figure 28. Visual assessments from crater repair testing – Crater 4.

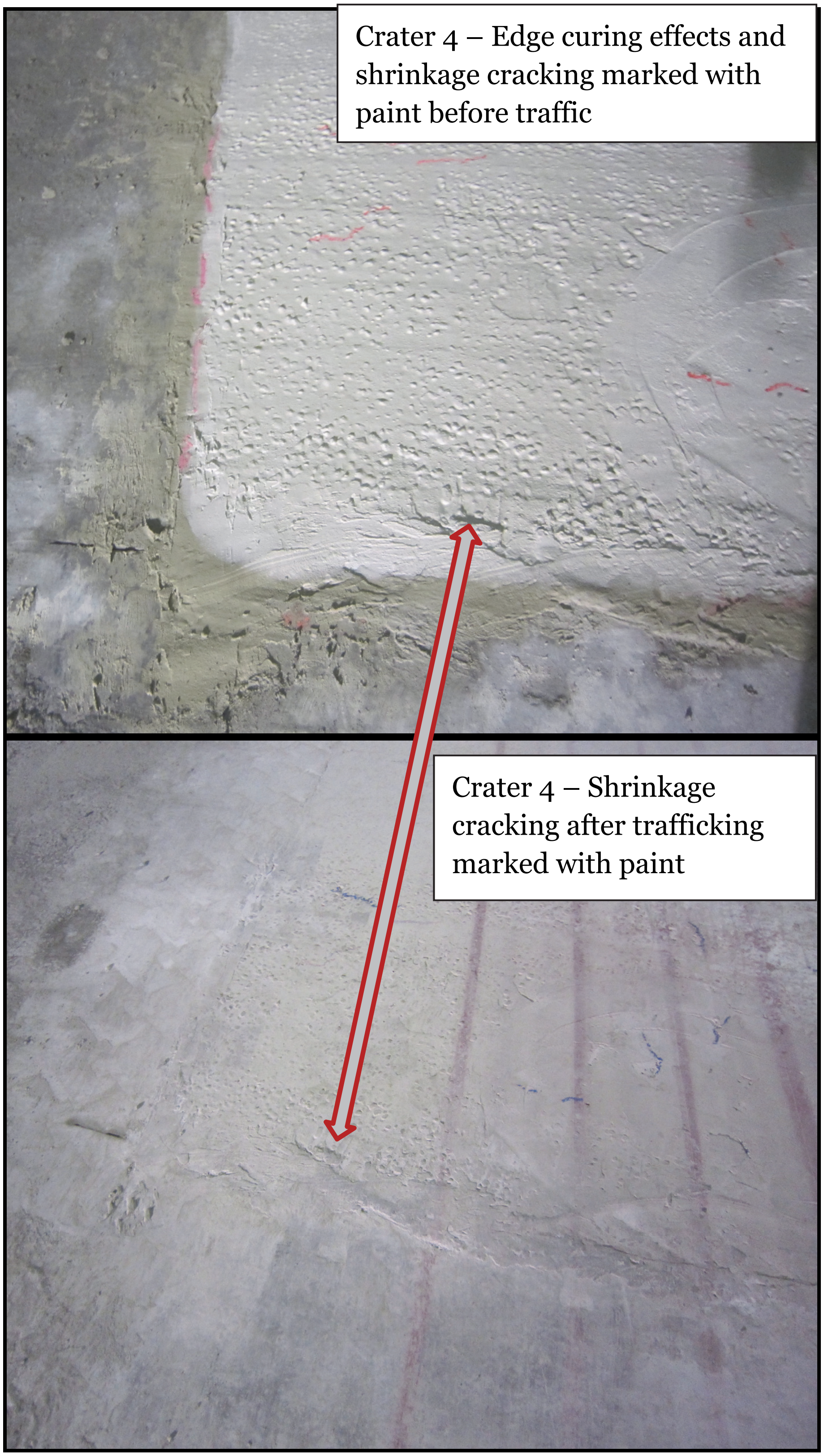

Figure 29. Visual assessment of Crater 5 just after placement.

A rod and level survey of the existing pavement in the area of Craters 1 to 4 (prior to producing Craters 1 to 4) showed that all elevations in this area were within 0.5 in. of each other. Rod and level surveys after trafficking the crater repairs showed that elevations were also within 0.5 in. of each other. Allowable USAF elevation changes are 1.25 in. for F-15E aircraft, but they reduce to 0.75 in. between the crater repair and surrounding pavement in terms of roughness requirements (USAF 1992). All measurements were within the 0.75-in. requirement, indicating no surface profile issues with any of these crater repairs.

3.3 Heavy weight deflectometer (HWD) test results

Table 7 contains HWD test results. Measured deflections for Crater 1 are questionable. Such low values for a material that had no heated water are unlikely. Craters 3 and 4 have comparable deflections. Craters 3 and 4 did not show any signs of structural degradation in the 112 simulated aircraft passes.

Crater 5 (flowable fill only) experienced very high deflections, as expected. Deflection directly under the HWD load plate (D_1) was approximately 69 mils, but 12 in. over at D_2, deflections had decreased drastically to approximately 12 mils. A deflection basin reducing by a half order of magnitude in 12 in. would not be expected unless the HWD drop damaged the flowable fill directly under the load. This is also evidenced by deflections at D_2 being around half of those measured on Craters 3 and 4, even though a smaller load was used for Crater 5. The RSC capped repairs would be expected to be as stiff as or stiffer than a DPFF layer 12 in. from the load, which is not what the readings from Crater 5 indicated. DCP readings support DPFF having more modest levels of stability with composite CBR values ranging from 13 to 42 at 30 to 80 min after curing (values generally increased with cure time).

Table 7. HWD test results.

Crater	Passes or Time	Stress (psi)	*Adj* Deflections (mils)						
			D_1	D_2	D_3	D_4	D_5	D_6	D_7
1	0 Passes	500	6.0	5.0	4.6	4.1	3.7	3.1	2.6
	112 Passes	500	6.2	4.8	4.3	3.9	3.5	3.0	2.7
3	0 Passes	500	26.6	21.0	13.3	6.4	4.0	3.5	3.0
	112 Passes	500	20.0	16.6	12.5	7.3	3.6	3.1	2.7
4	0 Passes	500	25.3	24.5	19.2	13.7	8.0	4.5	3.5
	112 Passes	500	26.9	22.3	15.6	8.8	5.1	4.3	3.6
5	2 hours	200	67.3	10.5	2.7	1.6	1.5	1.4	1.3
	12 hours	200	70.7	12.7	3.2	2.7	2.4	1.5	1.4

Note: No data were collected for Crater 2 since the flowable fill did not set. The top layer of Crater 5 was DPFF, while the remainder of the craters had a RSC cap.

3.4 Strength and setting assessments

Representative setting and strength gain measurements of rapid-setting materials at very early ages are useful but fairly challenging for cold weather placements. Specimen size effects are impactful when trying to use laboratory measurements to replicate properties of craters cast in situ, especially considering the temperature gradients likely to exist in a crater repair with VMFF cast in cold regions. This section documents unconfined compressive strength (UCS), set time (t_{set}), and CBR values from DCP measurements on VMFF in the very early stages of hydration.

Table 8 shows temperatures of the backfill and cap dry material and mix water measured prior to placement, along with the air temperature during placement of each. The mix water temperatures correspond with the test plan provide in Table 2. Dry material temperatures ranged from 36 to 46°F and air temperatures were all at or below 32°F.

Table 8. Material, water and air temperatures.

Crater	Backfill Dry Material	Cap Dry Material	Backfill Mix Water	Cap Mix Water	Backfill Air Temp	Cap Air Temp
1	46	39	57	57	30	32
2	37	---	52	---	27	---
3	39	39	80	57	27	29
4	37	36	87	57	31	29
5	37	---	91	50	30	32

Note: Temperature units are in °F

Compressive strength measurements on molded cylinders collected during backfill placement (Figure 24) were not productive. UCS strength from the cylinders averaged approximately 20 psi after 4 hr of cold curing, with no measurement exceeding 50 psi. FERF temperatures where the cold region repairs were performed ranged from 29 to 32°F, and temperatures in the adjacent MEF facility were 20 to 22°F. When these values are compared to the Figure 30 T_{FF} temperatures measured in the repairs themselves (Figure 23), differences are apparent. Figure 30 shows the temperatures measured during and after the flowable fill placement. Negative time values indicate temperature measurements taken during placement, and the positive time values indicate time lapsed after the flowable fill placement was finished.

Figure 30. Flowable fill temperature results.

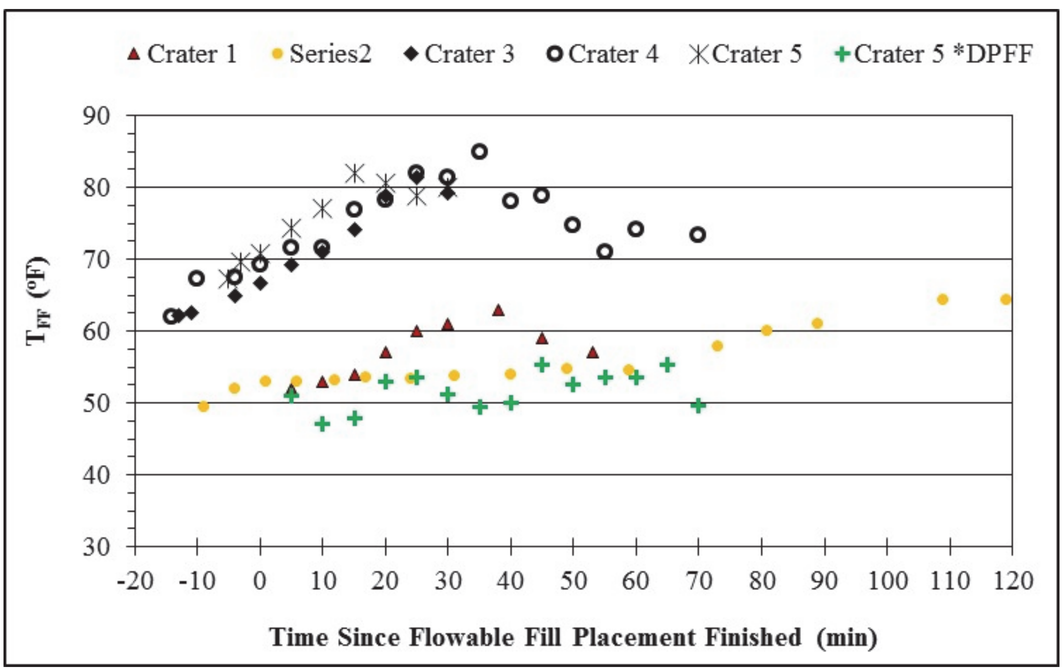

Craters 1 and 2 did not use heated water, and their temperatures were 50 to 64°F (Figure 30). Craters 3 to 5 did use heated water, and their temperatures were 62 to 85°F. When these values are compared to the MEF/FERF temperatures of 20 to 33°F and the small size of the molded cylinders are considered, it is apparent that the temperature condition of the molded cylinders is not representative of the conditions of the larger repairs. The larger repairs benefit from exothermic heat generation from cement hydration. Therefore, measuring properties on small molded specimens in order to represent properties present in the actual repair need to consider exothermic heat generation in the curing protocol for very early-age testing (e.g., 1 to 4 hr). Obtaining core samples directly from the crater repair could be a more effective way of measuring early-age properties of RSFF or RSC in sub-freezing temperatures. When viewing Figure 30, it should be noted that these temperatures were in the upper portion of the crater (a noticeable distance from an edge). Temperatures closer to the middle of the crater would be expected to be higher than those in Figure 30; DCP measurements presented later in this section show CBR values increasing with depth.

Limited set time data were collected. For Crater 1, t_{set} for the small molded cylinders was 2.6 hr when flowable fill was cured in the FERF (temperature near 33°F for this case). For Crater 1, t_{set} for the small molded cylinders was 2.9 hr when flowable fill was cured in the MEF (temperature near 22°F for this case). Comparably, the VMFF set time noted for Craters 1, 3, 4, 5 were approximately 45, 25, 25, and 28 min, respectively. The DPFF in Crater 5 had a set time of approximately 30 min.

As noted previously, the small UCS specimens had difficulty setting, while the large placements (Crater 2 being an exception) were able to set in 45 min or less. The large repair mass and the exothermic nature of rapid-setting cements made for a warmer temperature environment in the mass (especially the center of the mass) than in the small cylinders that were cured surrounded by cold air after casting. There were cases where the material in the repair had clearly achieved initial set, but the cylinders were still in a fluid state. As noted earlier in the report, visual observations of crater edges suggested they were softer than the interior due to temperature gradients. Crater 1's edges were noted to be softer than Craters 3 to 5, which is logical considering Crater 1 did not use heated mix water.

Table 9 summarizes CBR values estimated from DCP testing of VMFF as placed in the craters. CBR values were estimated at three depth intervals (0 to 6 in., 6 to 12 in., and 12 to 18 in.) and a composite CBR of this 18-in. depth was also determined by averaging the three values. Values below a depth of 18 in. were not considered since, as shown in Table 5, backfill thicknesses were 22 in. or less, and survey results showed crater bottom elevations were variable. Crater 5 values were not reported for lower depths (11 to 18 in.) since the backfill was only 12 in. deep.

Table 9. VMFF backfill CBR values estimated from DCP testing.

Crater	Cure Time (min)	CBR			
		0- to 6-in. Depth	6- to 12-in. Depth	12- to 18-in. Depth	Composite Value
1	30	1	2	15	6
1	40	1	1	1	1
1	50	5	20	20	15
1	60	15	45	65	42
1	70	20	70	50	47
3	30	10	30	25	22
3	40	10	20	55	28
3	50	10	50	65	42
3	60	30	60	90	60
4	30	1	3	5	3
4	40	3	6	8	6
4	50	8	10	20	13
4	60	12	25	7	15
4	70	18	35	45	33
4	80	20	32	45	32
4	90	20	45	60	42
5	30	23	15	---	19
5	40	35	15	---	25
5	50	30	20	---	25
5	60	35	15	---	25
5	70	40	40	---	40

Notes: Crater 2 did not set after 150 min – useful readings were not obtained. Crater 5 values were at 6- to 10-in. depth, instead of 6 to 12 in.

CBR values estimated from DCP testing provided evidence of meaningful strength property gradients with depth within as-placed VMFF. As noted earlier, in-plane strength property gradients are believed to decrease as crater edges are approached. For Crater 1, average CBR values of VMFF over time with depth were 8 (upper 6 in.), 28 (6- to 12-in. depth), and 30 (12- to 18-in. depth). Values were averaged in this manner to show that the strength properties in the upper 6 in. are much less than they are with depth. In a similar manner, the CBR values of Crater 3 were 15, 40, and 59 with depth, and Crater 4's CBR values were 12, 22, and 27 with depth. Strength property increases with depth within VMFF craters supports the previous discussion in this section about the challenges in characterizing as-placed VMFF in cold regions and that temperature conditions are a first-order factor in this process.

All repairs (with exception of Crater 2, which did not set) demonstrated variable setting tendencies over the 1.5-hr timeframe, during which strength was monitored. Crater 1 performed in an acceptable manner, but it did gain strength more slowly than what is typically observed in milder conditions or with heated water and would require a longer cure time to achieve the desired properties to return a pavement to service for aircraft traffic.

Table 10 summarizes CBR values estimated from DCP testing of DPFF for the top layer of Crater 5. As with the previous table, CBRs were estimated at three depth intervals, and a composite of this 18-in. depth was calculated. CBR values for the DPFF were comparable to CBR values from the VMFF but appeared to be more variable due to the inherent variability from the dry-placement procedure.

Table 10. DPFF CBR values estimated from DCP testing.

Crater	Cure Time (min)	CBR			
		0- to 6-in. Depth	6- to 12-in. Depth	12- to 18-in. Depth	Composite Value
5	30	5	17	17	13
5	40	10	30	12	17
5	50	8	20	30	19
5	60	15	70	40	42
5	70	17	23	---	20
5	80	15	40	23	26

The CBR values for all repairs are plotted as a function of time and are shown in Figures 31, 32, and 33 for 0- to 6-in. depth, 6- to 12-in. depth, and 12- to 18-in. depth, respectively. CBR values for Craters 1, 3, and 4 clearly show that heating mix water was more useful than use of $AlSO_4$. All three craters were tested at 30 and 60 min with a DCP, and those readings show that heated mix water made considerable improvements at 30 min, noticeable but lessened improvements at 60 min, and that $AlSo_4$ hindered strength gain even in the presence of heated mix water. Crater 1 was the control section and did not use heated mix water or $AlSO_4$. At 30 min, Crater 3 (heated mix water only) had a composite CBR value over 3 times that of Crater 1, while Crater 4 (heated mix water and $AlSO_4$) had half the CBR value of the control. At 60 min, Crater 3 had a composite CBR roughly 1.4 times the control, while Crater 4 had a composite CBR value roughly one-third of the control. By 90 min of cure time, Crater 4 was comparable to Crater 1 after only 60 min of cure time, i.e., there is evidence that AlSO4 hindered set time. All testing documented in this report showed AlSO4 reducing the performance of crater repairs in cold regions and Crater 3 (heated mix water only) being the best performing option evaluated.

Figure 31. DCP results (0- to 6-in. depth).

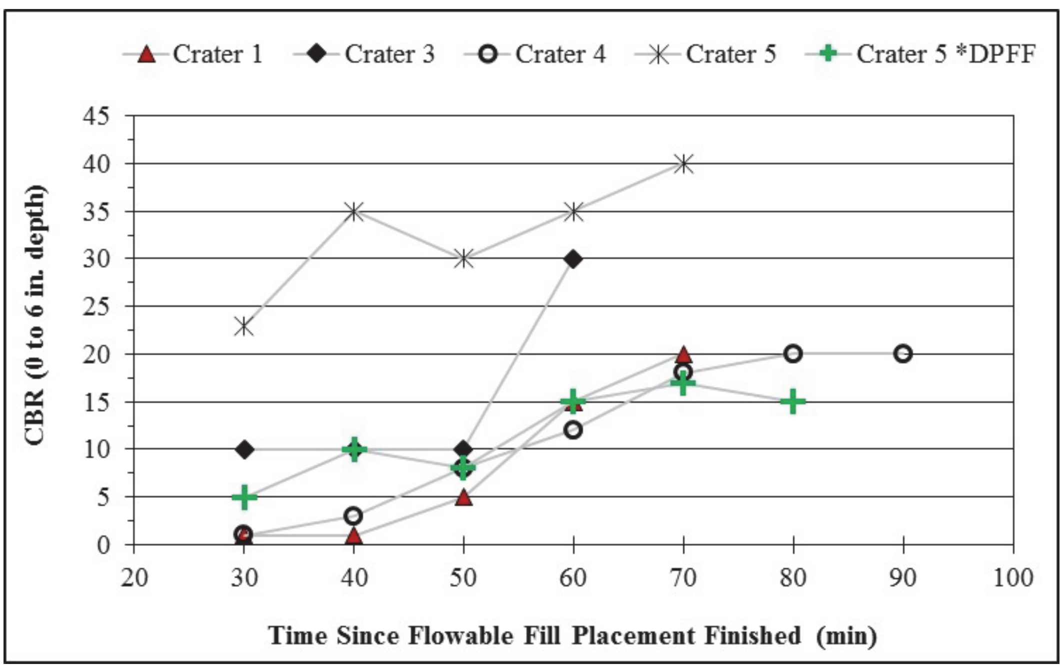

Figure 32. DCP results (6- to 12-in. depth).

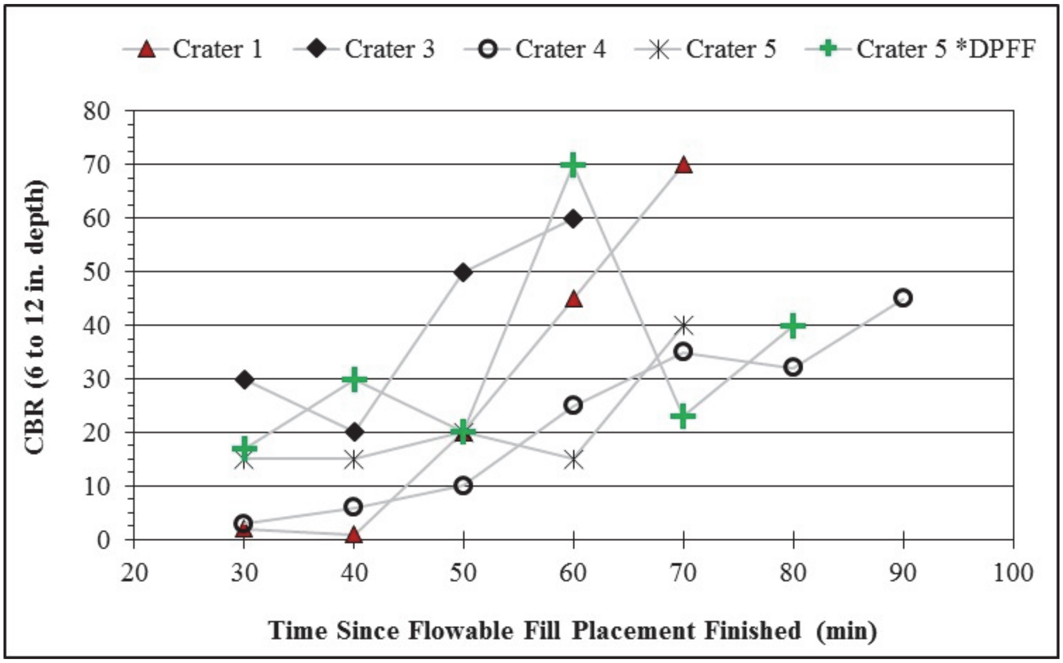

Figure 33. DCP results (12- to 18-in. depth).

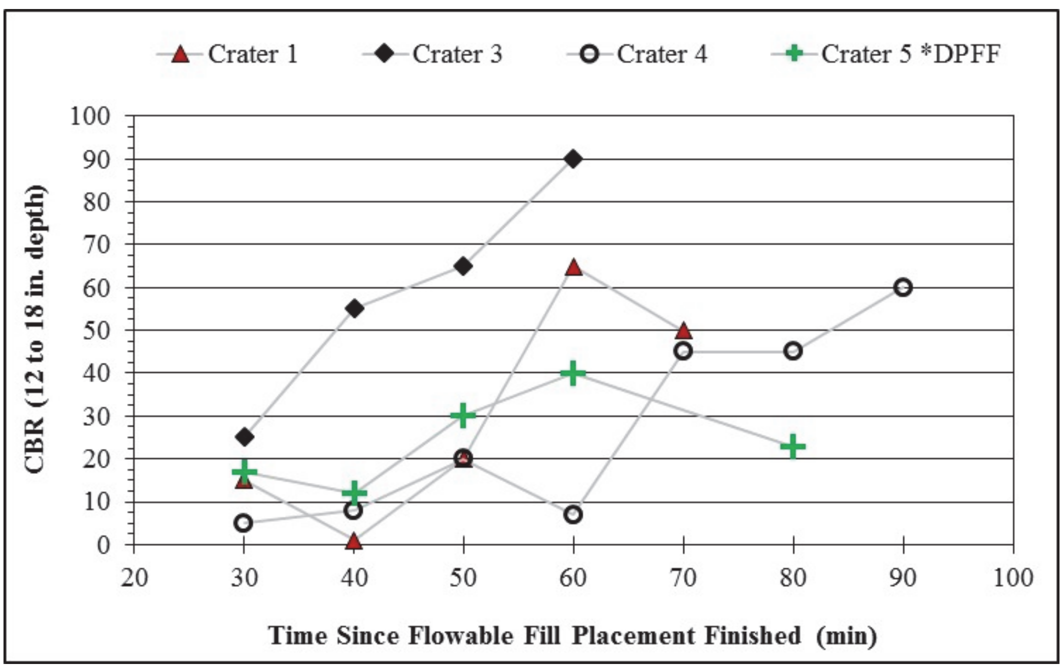

4 Summary and Conclusions

Results presented in this report showed that VMFF can be used as backfill under RSC caps in cold regions for expedient pavement repairs. Specific observations and conclusions are as follows.

1. Placement of VMFF in cold weather with traditional techniques used in moderate climates, i.e., no additives or heated mix water, performed in an acceptable manner and was able to withstand over 100 passes of simulated F-15E aircraft after 2 hr of cure time.
2. $AlSO_4$ did not perform in an acceptable manner. Flowable fill with $AlSO_4$ reduced performance relative to VMFF produced using standard methods.
3. Heating the mix water was the best method identified for cold region pavement repairs. Repairs incorporating heated mix water were able to withstand over 100 passes of simulated F-15E aircraft at early ages. Early-age strength property measurements suggested heated mix water to be a better alternative than placement in the traditional manner for moderate climates.
4. The immersion heaters added to the simplified volumetric mixer were successful and are performance improvements in cold weather conditions.
5. Other than heated mix water, no major procedural modifications were identified for crater repair in sustained cold weather, which is consistent with findings reported in Edwards et al. (2013).
6. Future work should consider further evaluation of manners in which to better characterize early-age properties of as-placed VMFF in cold regions. Challenges were identified for use of molded specimens, and data collected suggested a maturity or equivalent age concept for assessing the three-dimensional exothermic temperature profile of a crater repair might be useful. Data collected suggested that there are three-dimensional property gradients that are believed to be caused by the variation in curing temperature within a repair. This could be a productive area of future study, especially considering crater repair edges were identified as a particularly susceptible area. Edges often are the limiting factor in rapid pavement repair performance.
7. A full-scale asphalt test section is recommended to determine the set time required for both VMFF and DPFF to achieve proper asphalt density during compaction.

References

American Society for Testing and Materials (ASTM). 2004a. Standard test methods for density of soil and soil-aggregate in place by nuclear methods (shallow depth). C2922. In *Annual book of ASTM standards*. West Conshohocken, PA: American Society for Testing Materials.

_______. 2004b. Standard test method for water content of soil and rock in place by nuclear methods (shallow depth). D3017. In *Annual book of ASTM standards*. West Conshohocken, PA: American Society for Testing Materials.

_______. 2008. Standard test method for time of setting of concrete mixtures by Penetration Resistance. C403. In *Annual book of ASTM standards*. West Conshohocken, PA: American Society for Testing Materials.

_______. 2009. Standard test method for use of the dynamic cone penetrometer in shallow pavement applications. D6951. In *Annual book of ASTM standards*. West Conshohocken, PA: American Society for Testing Materials.

_______. 2012. Standard test method for compressive strength of cylindrical concrete specimens. C39. In *Annual book of ASTM standards*. West Conshohocken, PA: American Society for Testing Materials.

Anderton, G. L., and C. A. Gartrell. 2005. *Rapid maximum-on-ground (MOG) enhancement technologies*. ERDC/GSL TR-05-2. Vicksburg, MS: U.S. Army Engineer Research and Development Center.

Carruth, W. D., and I. L. Howard. 2016. *Evaluation of flowable fill surface performance*. ERDC/GSL TR-16-33. Vicksburg, MS: U.S. Army Engineer Research and Development Center.

Edwards, L., H. P. Bell, W. D. Carruth, J. R. Griffin, and J. S. Tingle. 2013. *Cold weather crater repair testing at Malmstrom Air Force Base, Montana*. ERDC/GSL TR-13-32. Vicksburg, MS: U.S. Army Engineer Research and Development Center.

Oren, J. I., R. D. Moser, V. Boddu, C. A. Weiss, and J. Clausen. 2014. *Laboratory evaluation of expedient low-temperature admixtures for runway craters in cold weather*. ERDC/GSL TR-14-10. Vicksburg, MS: U.S. Army Engineer Research and Development Center.

Priddy, L. P., J. S. Tingle, J. R. Griffin, M. C. Edwards, and T. J. McCaffrey. 2013a. *Critical Runway AssessmenT and Repair (CRATR) technology demonstration: Operational utility assessment (OUA), Avon Park Air Force Range, Florida*. ERDC/GSL-13-33. Vicksburg, MS: U.S. Army Engineer Research and Development Center.

Priddy, L. P., J. S. Tingle, M. C. Edwards, J. R. Griffin, and T. J. McCaffrey. 2013b. *Critical Runway AssessmenT and Repair (CRATR) technology demonstration: Limited operational utility assessment 2 (LOUA2), Tyndall Air Force Base, Florida*. ERDC/GSL-13-39. Vicksburg, MS: U.S. Army Engineer Research and Development Center.

Tingle, J. S., L. P. Priddy, C. Gartrell, M. Edwards, and T. J. McCaffrey. 2009. *Critical Runway AssessmenT and Repair (CRATR) limited operational utility assessment 1 (LOUA1), Tyndall Air Force Base, Florida*. ERDC/GSL TR-09-12. Vicksburg, MS: U.S. Army Engineer Research and Development Center.

U.S. Air Force (USAF). 1992. *Crushed-stone crater repair and line-of-sight profile measurement for rapid runway repair*. TO 35E2-5-1. Washington, DC: U.S. Air Force.

REPORT DOCUMENTATION PAGE

Form Approved OMB No. 0704-0188

1. REPORT DATE *(DD-MM-YYYY)* August 2018

2. REPORT TYPE Final

3. DATES COVERED *(From - To)*

4. TITLE AND SUBTITLE

Rapid-Setting Flowable Fill Performance in Cold Weather for Airfield Damage Repair

5a. CONTRACT NUMBER

5b. GRANT NUMBER

5c. PROGRAM ELEMENT NUMBER

6. AUTHOR(S)

Lulu Edwards, William D. Carruth, Jeb S. Tingle, and Isaac L. Howard

5d. PROJECT NUMBER 397483

5e. TASK NUMBER

5f. WORK UNIT NUMBER

7. PERFORMING ORGANIZATION NAME(S) AND ADDRESS(ES)

Geotechnical and Structures Laboratory
U.S. Army Engineer Research and Development Center
3909 Halls Ferry Road
Vicksburg, MS 39180-6199

8. PERFORMING ORGANIZATION REPORT NUMBER

ERDC/GSL TR-18-26

9. SPONSORING / MONITORING AGENCY NAME(S) AND ADDRESS(ES)

U.S. Air Force Civil Engineer Center
139 Barnes Drive, Suite 1
Tyndall AFB, FL 32403

10. SPONSOR/MONITOR'S ACRONYM(S)

AFCEC

11. SPONSOR/MONITOR'S REPORT NUMBER(S)

12. DISTRIBUTION / AVAILABILITY STATEMENT

Approved for public release; distribution is unlimited.

13. SUPPLEMENTARY NOTES

14. ABSTRACT

This report documents the repair process of five craters in cold weather utilizing rapid-setting flowable fill (RSFF) and rapid-setting concrete (RSC). The work discussed herein supports the Rapid Airfield Damage Recovery (RADR) Program, in which the main objective is to develop capabilities to rapidly repair damaged airfield pavements for the full spectrum of operational scenarios. The purpose of this report is to document constructability, to collect early-age properties pertinent to the ability of these crater repair techniques to carry aircraft traffic, and to measure performance by exposing crater repairs to simulated aircraft traffic. Crater repair testing occurred at the Frost Effects Research Facility at the ERDC Cold Regions Research and Engineering Laboratory in Hanover, NH. Results showed RSFF could be a suitable cold-weather backfill. Aluminum sulfate was tested as an additive for use in cold weather, but repairs utilizing it did not perform well. The most efficient manner of using RSFF in cold weather was to heat the mix water. With heated mix water, a rapidly placed pavement repair was able to withstand 100 passes of an aircraft load cart after approximately 2 hr of cure time where RSFF was the backfill and RSC was the cap.

15. SUBJECT TERMS (see reverse)

16. SECURITY CLASSIFICATION OF:			17. LIMITATION OF ABSTRACT	18. NUMBER OF PAGES	19a. NAME OF RESPONSIBLE PERSON
a. REPORT	b. ABSTRACT	c. THIS PAGE			19b. TELEPHONE NUMBER *(include area code)*
Unclassified	Unclassified	Unclassified		60	

15. SUBJECT TERMS (concluded)

Flowable fill
Cold weather
Immersion heater
Rapid-setting concrete repair
Rapid airfield damage recovery
Concrete additives
Runways (Aeronautics) – Maintenance and repair
Runways (Aeronautics) – Cold weather conditions
Pavements – Performance
Aluminum sulfate
Heavy vehicle simulators